





Experimental study of the roughness variation of friction stir welding FSW

Azzeddine Belaziz ¹ ✉, Mohamed Bouamama ¹, Imane Elmeguenni ¹,
Samir Zahaf ²

¹ Mechanics Research Center (CRM), BP N73B, Ain El Bey, 25021 Constantine, Algeria

² Department of Technology, University of Djilali Bounaama-Khamis Meliana, Road Théniet El had, 44225,
Algeria

✉ belaziz2013@gmail.com

Abstract. The use of the Friction Stir Welding (FSW) process in aircraft construction, naval or nuclear reduces manufacturing costs and indirectly, operating costs through structural lightening. The aluminum alloys have very interesting specific properties such as very good electrical and thermal conductivity, good ductility accompanied by good mechanical and corrosion resistance. It is for this reason that these alloys are used in many industrial sectors. The aluminum based alloys are difficult to melt weld due to their high thermal conductivity and oxidation rate at temperatures very close to that of melting. The purpose of this investigation is to study the variation of the surface roughness on the weld joint of 5 mm thick plates of AA6061-T6 using friction stir welding FSW and carried out using a simple form pin tool. Surface roughness of FSW joints as a function of welding parameters (rotational speed, welding speed). The surface roughness of FSW joints has a big impact on the fatigue of the welded joint, hence determining the minimum surface roughness is critical. The quality of an FSW joint is heavily influenced by the tool and welding settings. The tool's geometry affects both the heat distribution and the amount of metal entrained by the tool. This paper provides outcome of impact of welding parameters on microhardness, and surface roughness of friction stir welded AA6061- T6. Conclusions derived from this research work are: the FSW joint's microstructural examination reveals homogeneous particle distribution.

Keywords: FSW process, Rotational speed, Welding speed, microscopic, microhardness, surface roughness.

Citation: Belaziz A, Bouamama M, Elmeguenni I, Zahaf S. Experimental study of the roughness variation of friction stir welding FSW. *Materials Physics and Mechanics*. 2023;51(3): 115-125. DOI: 10.18149/MPM.5132023_13.

Introduction

The AA6061 aluminium alloy has Highly resistant to corrosion in the marine environment, as well as moderate mechanical qualities and high fatigue-fracture resistance. It offers good formability, machinability, and weldability when used in arc or resistance welding procedures (metal inert gas – MIG or tungsten inert gas – TIG) [1,2]. The TWI pioneered the friction stir welding (FSW) technology in 1991, and it is undoubtedly the most amazing and possibly valuable new welding technique. The originality of this process consists in welding in the solid state, which eliminates the defects linked to solidification and leads to low internal stresses compared to conventional welding (laser or arc welding). The FSW is well suited to the fabrication of sheet assemblies in Aluminum or its alloys that are difficult to weld using standard methods (MIG, MAG, TIG, etc.). Defects in FSW welded joints substantially impair the joint's mechanical characteristics. Within the weld, there are several zones where the

microstructural evolution is governed by the complex interaction of plastic deformation, restoration, recrystallization, and homogeneous and heterogeneous precipitation. The FSW is performed using a punch with a shoulder and a pin. The tool rotates while applying pressure to the plates' surface during welding. Heating from friction between the tool and the workpiece, as well as plastic work dissipation at high strain rates created by tool pin stirring the materials, is used to soften the materials and form joints during the friction stir welding (FSW) process [3–6]. Currently, FSW research is mostly focused on the weld material; however, while a number of materials, such as aluminum, have achieved significant success, research on the friction stir tool is still in its infancy [7–16]. The heat generation and flow of the plastic material are affected by the pin's shape. Eventually, the pin will have an impact on the weld's form, mechanical qualities [17–19] and on the surface roughness of the joint. Residual stress in friction stir weld (FSW) joint significantly affects fatigue performance [20].

In this study, the surface roughness of FSW joints has a big impact on the fatigue of the welded joint, hence determining the minimum surface roughness is critical. The quality of an FSW joint is heavily influenced by the tool and welding settings. Surface roughness of FSW joints as a function of welding parameters (rotational speed, welding speed). The purpose of this investigation is to study the variation of the surface roughness on the weld joint of 5 mm thick plates of AA6061-T6 using friction stir welding FSW and carried out using a simple form pin tool. The feed rate, the tool's rotational speed, the distance between the pin and the joint's root, the tool's vertical force, and the inclination of the shoulder with regard to the joint's surface are all process parameters that influence the seal's quality. The roughness of a 120 mm long weld connection was measured in five portions for this study. The starting and ending parts of the welding tool are given special attention.

In order to decouple the different phenomena. The surface properties can have an impact on the mechanical behavior of the weld joint [21]. The quality of the surfaces is largely dependent on their roughness. Technically, it is important to determine the roughness of the weld joint to control the smooth surface.

Experimental Procedure

Materials. In this study, we used two types of materials. The first is intended for the FSW welding operation, we used a high alloy steel tool which bears the designation XC48 steel. The alloys were purchased in the form of rolled plates of 5 mm thick. The nominal chemical compositions of the parent material XC48 steel are listed in Table 1. Moreover, the tensile strength, yield strength, elongation and Hardness of the parent materials are summarized in Table 2. The second material studied is a AA6061-T6 aluminum alloy supplied in the form of 5 mm plates.

Table 1. Chemical composition of XC48 steel (mass percent, %)

C	S	Mn	P	Si
0.42	0.029	0.7	0.042	0.38

Table 2. Mechanical properties of XC48 steel

Tensile strength, MPa	Yield strength, MPa	Elongation, %	Hardness (HV)
535	468	11.2	150

The material used for welded in the experiments was AA6061-T6. This type of aluminium alloys AA6061-T6 is widely used in the automobile, marine and aerospace industries as skin and structure applications for skin and structure. The standard EN-AW 6061 aluminum alloy with chemical composition in mass fractions: 0.80 % Si, 0.70 % Fe, 0.05 % Cu, 0.15 % Mn, 0.05 % Mg, 0.35 % Cr, 0.25 % Zn, 0.15 % Ti and the rest Al, and temper O, was used for

testing. The workpiece dimensions were $250 \times 100 \times 5$ mm. The physical and mechanical properties of the alloy for temper O were determined, taken according to the standard (Table 3).

Table 3. Mechanical properties of the aluminum alloy AA6061-T6

Aluminum Alloy	USS, MPa	YS, MPa	Elongation, %
AA6061-T6	308	278	13

FSW tool. The quality of a Stir friction welding FSW joint depends greatly on the tool and the welding parameters. The geometry of the tool is a determining factor in the heat distribution and the amount of metal driven by the tool. However, welding speed, rotational speed, the distance between the pawn and the root of the seal, the vertical force exerted by the tool and the inclination of the shoulder relative to the surface of the surface joint are processes of parameters that influence the quality of the joint. These parameters vary depending on the soldering metal, the joint configuration and the geometry of the tool used. They are normally determined experimentally after choosing the tool. The effect of the tool rotation speed is nonlinear on the mechanical properties [22].

The choice of the FSW tool was made from XC48 steel, the tool design is an important parameter in FSW processes, which influences the heat generation, the resulting microstructure and mechanical properties of the welded material. A basic FSW tool geometry was used with a pin, the resulting microstructure and mechanical properties of the welded material. The rotating tool was made of XC48 steel with a pin diameter of 4 mm, a pin height of 3.5 mm, and a shoulder diameter of 16 mm. An inclination angle of 2.5° was applied for the tool during the joining process and the formation of welds under the position-control mode. The configuration of the tool used in this study is shown in Fig. 1

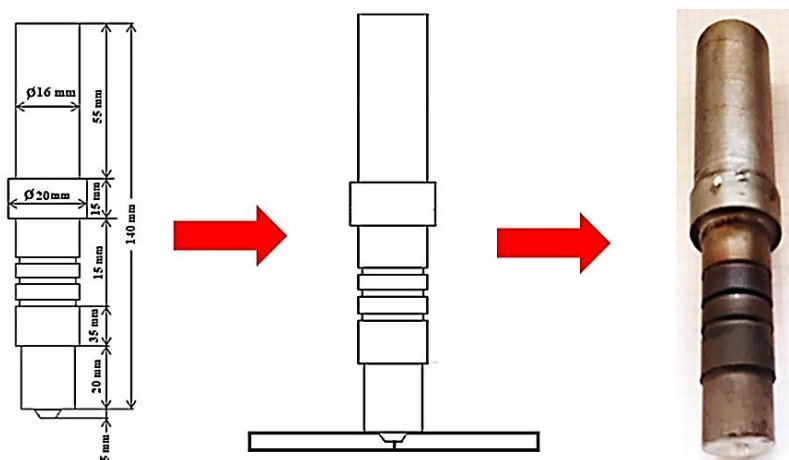


Fig. 1. Friction stir welding (FSW) tool used in the FSW experiments

The most important geometric parameter in the FSW tool design is the diameter of the shoulder, which is currently designed by test and error methods. The influences of the diameter of the shoulders on thermal cycles, the advanced temperatures, the power requirements and the torque during the FSW processes are complex and must still be resolved to be fully understood. A criterion for the design of a tool shoulder diameter based on the principle of the maximum use of the pair provided for traction has been proposed and tested.

Unconventional FSW, the tool is considered non-consumable. However, extreme welding conditions shorten its life and can quickly damage it. The material of the FSW tool used (XC48 steel) must ensure its resistance to the stresses exerted by the material. The active part of the tool degrades under the effect of the forces generated during the interaction tool /

tribology material and extreme thermal conditions. For each welding phase, the tool is subjected to different forces, which vary according to the operating conditions.

Friction Stir Welding Procedure. The welding process was performed on the vertical milling numerical machine. A plan of experiments was prepared regarding the capabilities of the universal milling machine used. The welding speeds have been precisely selected and tested at a constant inclination angle of 2.5° . Welding parameters (rotational speed of 1250 RPM and welding speed was 71 mm/min). The position of the tool with respect to the joint configuration is shown in Fig. 1.

The plates of the alloy AA6061-T6 were positioned and fixed in the fixation systems FS, the plate fixing system must withstand the forces which tend to separate and displace the parts to be assembled. The magnitude of these forces capable of deforming the upper surface of the welded plates.

Although the shoulder of the tool exerts an axial force to keep the tool resting on the support, it is the fixation system that must perform this function.

The generation of heat in the FSW process is the consequence of several physical phenomena. The heat sources induced by these phenomena can be classified as tool-part interaction. This interaction is the source of a surface heat flux at the tool-material interface. The surface to which the flux is applied can vary from a disk with a radius equal to that of the shoulder located on the upper face of the sheets to a more complex surface taking into account the angle of inclination of the shoulder and the pawn surface [23]. The heat flux can be calculated from the heat dissipated by friction [24] or from the total power supplied to the tool [25]. For these two cases, the coefficient must be determined experimentally of friction and the total power supplied to the tool. The heat necessary for the process is generated by the tool rotation and clamping (usually downward force) of the tool on the joint line [26]. Generally, the tensile shear load is primarily impacted by the tool penetration depth [27].

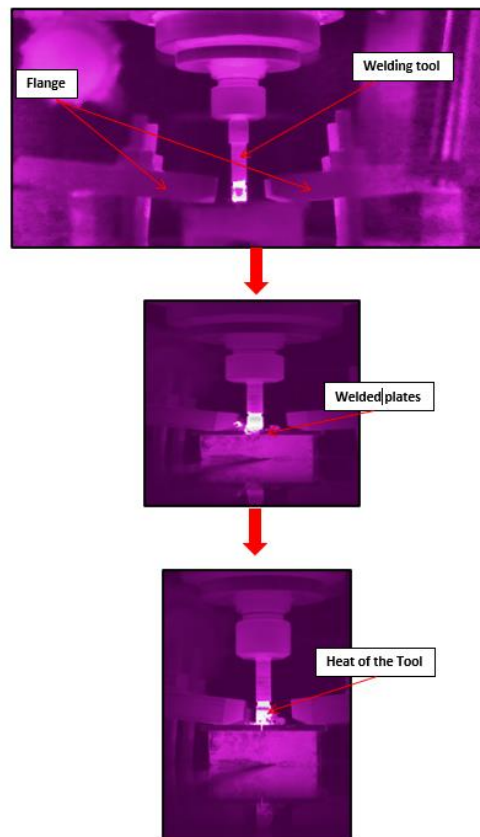


Fig. 2. Thermal observation

During welding, the highest temperatures are concentrated around the pin and under the shoulder (Fig. 2). Then, as you move away from the tool, the temperatures gradually decrease, until they fall back to ambient temperature. The plot of temperature versus position provides further detail on thermal fields.

Mechanical Properties (Hardness test). Using a universal hardness testing machine with camera and screen, NEMESIS 9001. We can see the evolution of the hardness on the cross-section of the welded joint. The Vickers hardness measurement is carried out using a standard diamond pyramidal tip with a square base and an apex angle between faces equal to 136° . The imprint therefore has the shape of a square; we measure the two diagonals d_1 and d_2 of this square using the camera and the screen of the same device. The value d is obtained by taking the average of d_1 and d_2 . It is d which will be used for the calculation of the hardness. The strength and duration of support are also normalized. For each weld joint, a sample was taken, so the advance side (AS) was chosen as the starting point for the measurement. The microhardness of different welded plates was measured according to the Vickers standard. A polishing is necessary before taking the microhardness measurements, to have a surface condition without any scratches likely to interfere with the penetration of the indenter.

Results and discussion

Visual inspection. From the FSW welds, the surface condition of welded plates is a first clue for estimating the quality of the welded joint. Respecting the welding protocol described in the previous section, a tool configuration has been devoted to arrive at a satisfactory surface finish to access the mechanical characterization. Figure 3 shows the surface condition of welded plate with a tool configuration we suggest. The welded plate exhibited burrs (called "flash") on the retreating side (RS) (Fig. 4), flash affects the surface finish of the weld and can be interpreted. In this experimental, the weld apices were smooth. The visual inspection observation cuts of the welded joints confirm that there are no internal defects (tunnel effect). After visual analysis of the welded joints, we can say we have a good weld seam and a good seam.

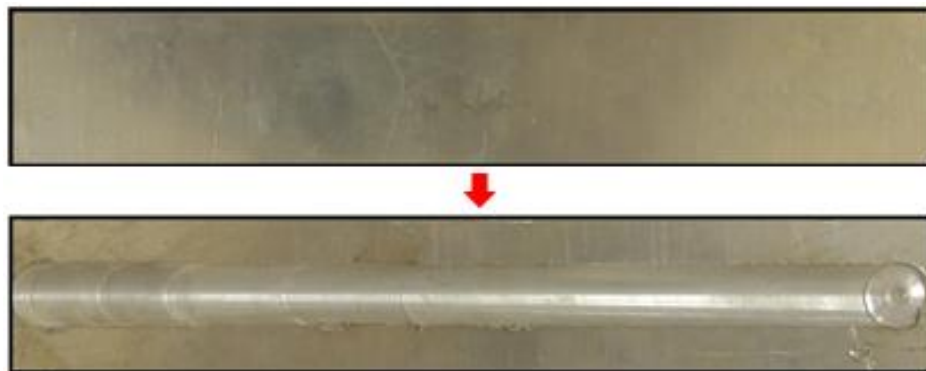


Fig. 3. Weld joints and joint bottoms for welding parameters

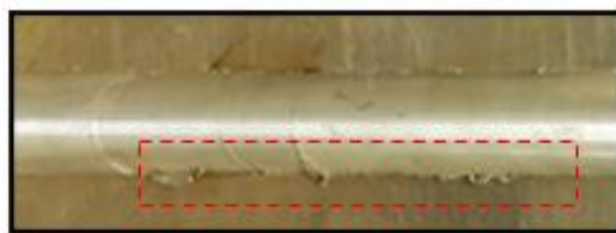


Fig. 4. Burrs after welding FSW.

Microscopic analysis. Monitoring and controlling the condition of surfaces is a major need for manufacturers. A new roughness parameter is proposed to quantify the smoothness of a surface independent of amplitude and units of sweep length. The effectiveness of this parameter is tested on periodic noisy surfaces with different degrees of anisotropy. The value of this parameter is between zero (perfect noise) and 100 %.

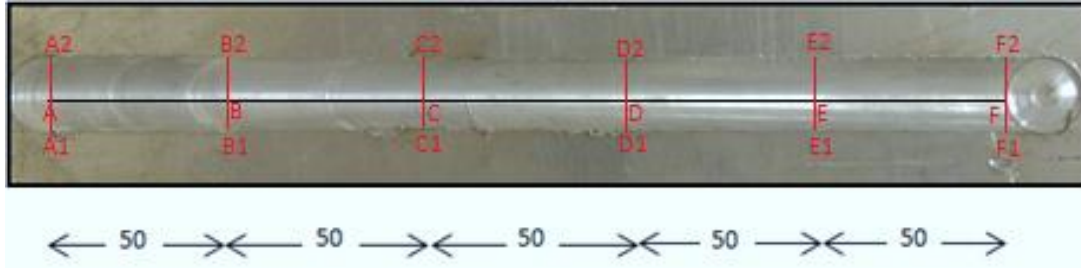


Fig. 5. Profile of roughness measurement points on the welded structure

It is clear from Fig. 5 that the surface condition of the weld joint has several defects which will weaken the behavior of the joint. We noticed excessive burrs and chippings in the form of scrap on the surface of the welded plates. FSW solder joint has intrinsic properties such as density, conductivity and modulus of elasticity; the surfaces representing the limits of the materials can be a little more insubstantial, but we still think of some of these properties as an intrinsic quality, however there are other properties which are easy to define but whose values seem to depend on technique or scale, measuring roughness, for example, seems to be a property with an additional difficulty that is not always easy to define as a concept.

The roughness measurement points on the welded structure and the distance between the points in this study are represented in the Fig. 5.

The different roughness parameter such as R_z is calculated on each profile resulting from the decomposition obtained. The evolution of the roughness parameter R_z with respect to the scale of the wavelet decomposition.

The feed rate has a greater influence on the microstructure of the joint than the rotational speed. The heat intake does not only depend on the distance traveled. It also depends on the welding power. A too high feed rate leads to the formation of cavities commonly referred to as tunnels or "wormholes" at the root of the joint. The feedback ratio defined by the coefficient between the feed rate and the speed of rotation is the main parameter that controls the presence and size of the cavities. The higher the high report, the more cavity training is favored. For advance speed, proposing ductility increase with increased speed of rotation. Excessive rotational speed causes the increase in the temperature of the joint and the formation of internal defects. The equivalent plastic deformation can be approximately correlated with the evolution of the microstructure.

Microstructure was studied with an optical microscope, while grains size was determined by Image J software (Fig. 6).

Figure 6 shows the welded joints subjected to microscopic inspection, when the welded joints were subjected to microscopic inspection, tiny scattered voids were observed in some more welded joints in the lower stir region toward the advancing side.

The grain size was found to be influenced by processing parameters. Weld microstructure displayed mixed structure comprising both the base metals, so it is imperative to study advancing and retreating sides.

Figure 6 ($A_1, B_1, C_1, D_1, E_1, F_1$) presents a micrograph of the first point of tool rotation, the weld is without defects, except for possible under fill, due to the higher heat input. The streaks are very small at the first points of the weld, which were in the vicinity of the tool shoulder. At

the middle of the weld root joint (Fig. 6), the surface roughness is clearly seen as a line. In this part (zone) the tool must provide both mixing and friction with the material to be welded. These functions quickly degrade the tool, the movement of the rotating material under the effect of friction at the tool / plate interface and in mixing due to the pin creates a source of plastic deformation. Therefore, most of the heat is created by the tool / plate's friction in the middle zone.

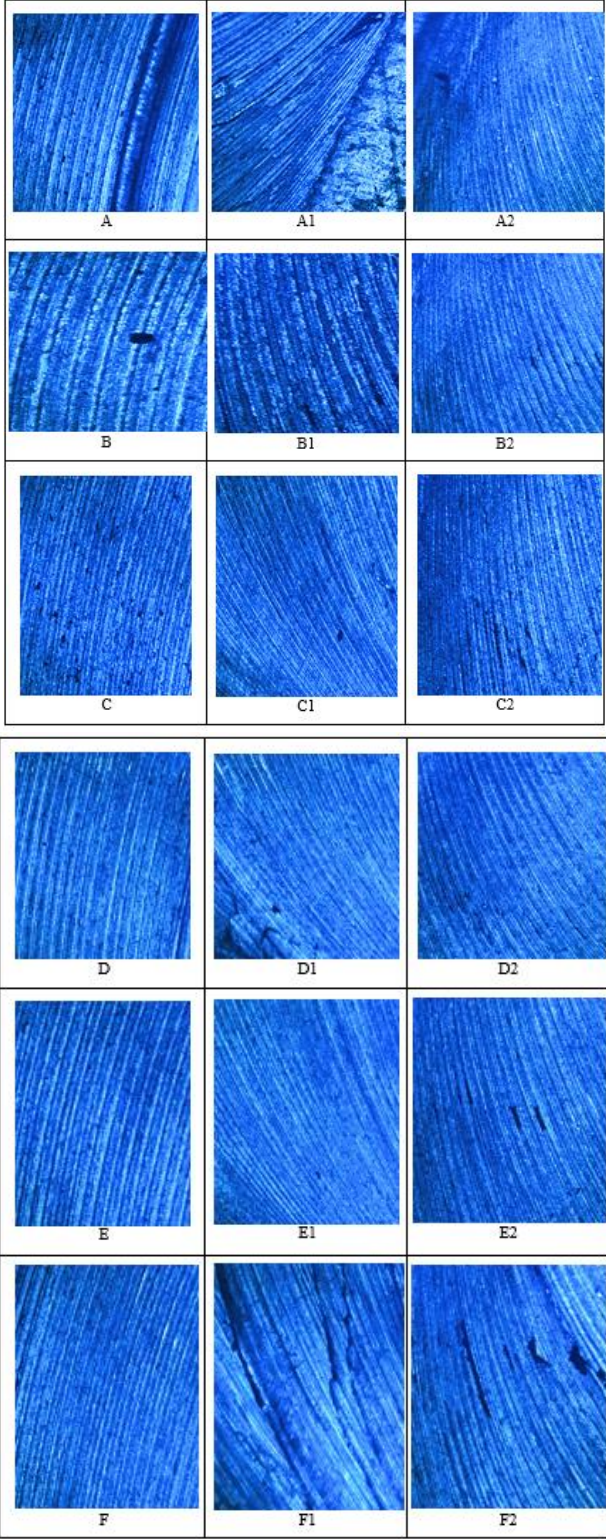


Fig. 6. Micrograph showing the surface condition and roughness measurement points

Figure 6 ($A_2, B_2, C_2, D_2, E_2, F_2$) presents a micrograph of the last point of the tool's rotation, the welding joint has some small flaws. Welding flaws are irregularities, discontinuities, blemishes, or inconsistencies in the weld surface of welded pieces. Weld joint defects can lead to part and assembly rejection, costly repairs, considerable reductions in performance under operating conditions, and, in the worst-case scenario and catastrophic failures.

Effects of surface roughness. Roughness R_z (μm): The surface roughness (Ra) of the weld joint was measured with instruments for the most diverse applications. From the present result (Fig. 7) it was confirmed that the welding parameters such as rotational speed and welding speed used are useful, that is, when surface roughness and contact force are changes from the experiments.

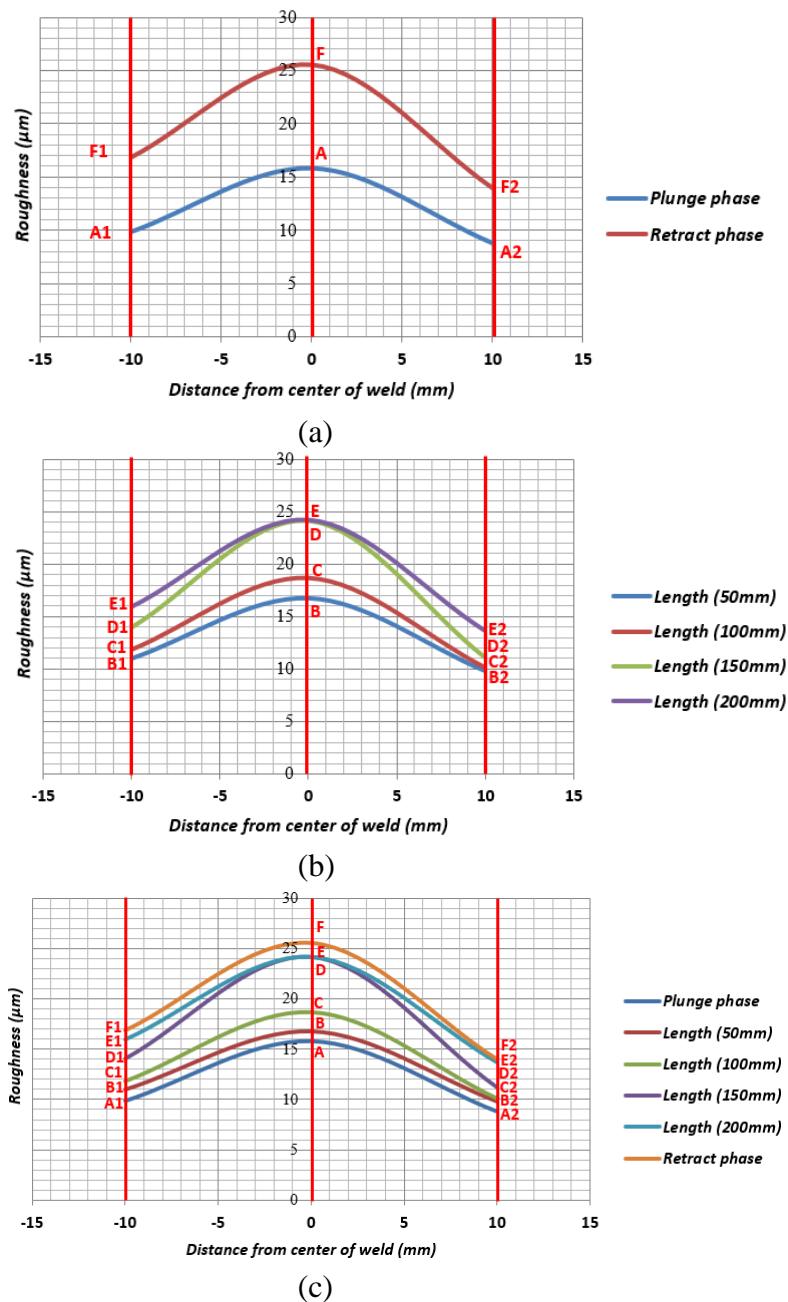


Fig. 7. The distribution Roughness (μm): (a) plunge and retract surface; (b) jointing surface; (c) all surface welding.

The obtained results demonstrated that spherical nano-sized grains of the joints were produced. Surface roughness aids in determining the integrity of the surface. The roughness of a surface also aids in determining its function. This is because a significant portion of material failure begins near the surface. It could be the result of a surface irregularity or decrease in quality. Corrosion resistance is also influenced by the surface finish. Surface finish enhances component performance while lowering component life cycle costs.

At the advancing side, the material flow on AS differs from the flow on RS. On the RS, AA6061-T6 should not be in the rotational zone near the pin. Surface roughness increases with rotational speed.

Since the roughness is taken as a factor of the surface profile to be considered in the estimation of the fatigue life of structures welded by FSW. Different roughness measurements were taken in the joint of AA6061-T6 welded by FSW on selected points as shown in Fig. 5.

The results show that within a AA6061-T6 alloy weld, the surface roughness values increase along the entire weld length as seen in Fig. 7, due to the shoulder penetration of the tool that necessarily affects the surface and causes ridges in the surface profile along the weld. The roughness R_z vary from start to finish (between 9.84 and 16.87 μm on the RS side, 8.77 and 13.98 μm on the AS side) and level off slightly towards the end as the heat input reaches its steady state.

We observed that the retreating side RS presents high values of roughness compared to the advancing side AS, this increase is explained by the heterogeneity of the weld joint FSW. In addition, the roughness is important at the level of the peaks resembling the welding center (nugget) where the level of deformation is very high.

This will have an effect on the areas of surface stress concentrations and the period of fatigue crack interaction.

Vickers Hardness examinations. The variation of the micro hardness of all areas on the sample Shown in Fig. 8. Minimum values of hardness were found at the regions of base metal BM with values varying from 50 to 52 HV and maximum peaked values were found at the core region at the contact surface with metals. Values changing from 62 to 64 HV. The microhardness test allows us to have information on the structural change of the weld joint and to identify the different areas. The test was carried out in the transverse plane through the assembly with a Vickers indenter. Figure 8 shows the hardness measurement points on a sample AA6061-T6 aluminum alloy.

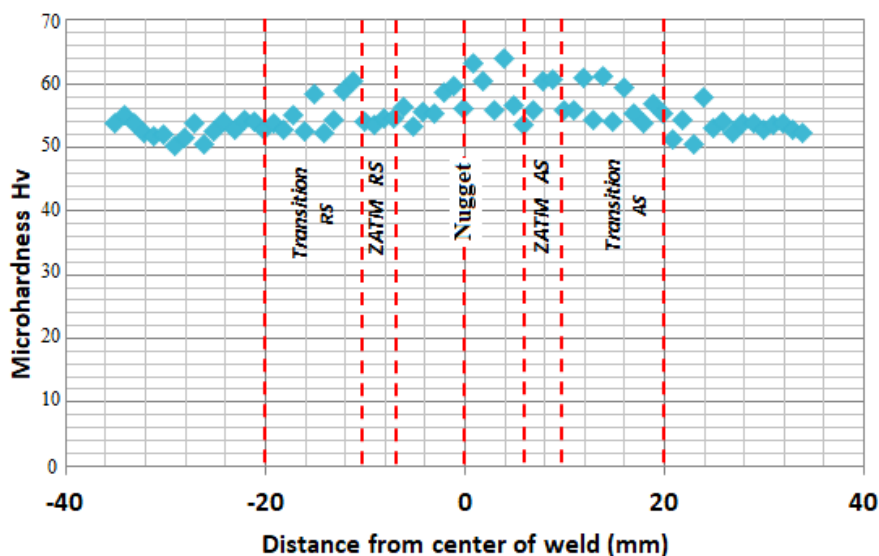


Fig. 8. Micro-hardness profile through a welded joint

The hardness profile (Fig. 8) clearly shows the influence of the microstructure on the hardness, the measurements in the different zones reflect the microstructure relating to each zone. It is noted that the hardness increases in the center of the nugget, this increase is explained by the refinement of the grains in this zone.

We notice that the hardness of the heat affected zone drops compared to the base metal BM (at around 50 HV), saw the coarsening of grains in this zone as well as the temperature reached by this zone generates the HAZ hardness gradient observed in Fig. 8.

A dispersion of hardness is noticed at the level of the thermomechanically affected zone, we explain this weakness by the plastic deformation in this zone induced by the FSW process, this zone is characterized by a strongly plastically deformed microstructure.

Conclusions

In order to achieve the main objective of this work, an experimental study of the FSW welding process is devoted. An experimental study was used in order to apply friction stir welding (FSW) and even the roughness of the welding joint under the effect of the welding parameters proposed by ourselves. This study clearly showed that there is a good agreement between the welding parameters chosen and the material to be used.

However, there are still several points to be explored as a perspective of this work, which we quote below:

Develop a digital model based on this thermomechanical model by inserting the pin into the welding tool.

The main conclusions are as follows:

- The increase in the speed of rotation causes an increase in the maximum temperature in the welded joints. Also, increasing the feed rate results in a decrease in the maximum temperature.
- All of the roughness prediction results found by this experimental part, we never reached the roughness of the weld joint in question.
- The shape of the tool is an important part of FSW welding. In the experimental welding, the tool with a taper of 2.5° gave very good results.
- The hardness profile is relatively symmetrical with respect to the parting line for the proposed welding parameters. The minimum hardness levels are achieved in the ZATM (RS) at around 52 HV. A slight level of hardness reaches a value of 64 HV, especially at the feed side (AS).
- The value of the microhardness in the ZATM for the proposed welding parameters can reach 60 HV is higher than that of the base metal which is 54 HV.

The microhardness test allows us to have information on the structural change of the weld joint and to identify the different areas. The test was carried out in the transverse plane through the assembly with a Vickers indenter. Figure 11 shows the hardness measurement points on a sample AA6061-T6 aluminum alloy.

References

1. Tusek J. Experimental investigation of gas tungsten arc welding and comparison with theoretical predictions. *IEEE Trans. Plasma Sci.* 2000;28(5): 1688.
2. Podrzaj P, Polajnar I, Diaci J, Kari` Z. Overview of resistance spot welding control. *Science and Technology of Welding and Joining.* 2008;13(3): 215.
3. Mishra R S, Ma Z Y. Friction stir welding and processing. *Materials Science and Engineering R.* 2005;50(1): 1-78.
4. Nandan R, DebRov T. Bhadeshia H K D H. Recent advances in friction stir welding process. weldment structure and properties. *Progress in Materials Science.* 2008;53(6): 980-1023.

5. Tuntum CC, Hattel JH. Numerical optimisation of friction stir welding: review of future challenges. *Science and Technology of Welding and Joining*. 2011;16(4): 318-324.
6. Rai R, De A, Bhadeshia HKDH, Debroy T. Review: friction stir welding tools. *Science and Technology of Welding and Joining*. 2011;16(4): 325-342.
7. Staron P, Koçak M, Williams S, Wescott A. Residual stress in friction stir-welded Al sheets. *Physica B: Condensed Matter*. 2004;15: E491-E493.
8. Hwa SP, Takahiro K, Taichi M, Yoshitaka N, Kazuhiro N, Masao U. Microstructures and mechanical properties of friction stir welds of 60% Cu–40% Zn copper alloy. *Materials Science and Engineering: A*. 2004;25: 160-169.
9. Olga VF, Christine K, Murr LE, David B, Sridhar P, Brook MN, McClure JC. Microstructural Issues in a Friction-Stir-Welded Aluminum Alloy. *Scripta Materialia*. 1998;38(5): 703-708.
10. Yutaka SS, Seung HCP, Masato M, Hiroyuki K. Constitutional liquation during dissimilar friction stir welding of Al and Mg alloys. *Scripta Materialia*. 2004;50(9): 1233-1236.
11. Won BL, Seung BJ. The joint properties of copper by friction stir welding. *Materials Letters*. 2004;58(6): 1041-1046.
12. Michael AS, Bangcheng YA, Reynolds P, Junhui Y. Banded microstructure in 2024-T351 and 2524-T351 aluminum friction stir welds: Part II. Mechanical characterization. *Materials Science and Engineering: A*. 2004;364(1-2): 66-74.
13. Liu HJ, Fujii H, Maeda M, Nogi K. Tensile properties and fracture locations of friction-stir-welded joints of 2017-T351 aluminum alloy. *Journal of Materials Processing Technology*. 2003;142(3): 692-696.
14. Charit I, Mishra RS. High strain rate superplasticity in a commercial 2024 Al alloy via friction stir processing. *Materials Science and Engineering: A*. 2003;359(1-2): 290-296.
15. Somasekharan AC, Murr LE. Microstructures in friction-stir welded dissimilar magnesium alloys and magnesium alloys to 6061-T6 aluminum alloy. *Materials Characterization*. 2004;52(1): 49-64.
16. Sharma SR, Ma ZY, Mishra RS. Effect of friction stir processing on fatigue behavior of A356 alloy. *Scripta Materialia*. 2004;51(3): 237–241.
17. Prado RA, Murr LE, Shindo DJ, Soto KF. Tool wear in the friction-stir welding of aluminum alloy 6061+20% Al₂O₃: a preliminary study. *Scripta Materialia*. 2001;45(1): 75-80.
18. Mustafa B, Adem K. The influence of stirrer geometry on bonding and mechanical properties in friction stir welding process. *Materials & Design*. 2003;25(4): 343-347
19. Prado RA, Murr LE, Soto KF. Self-optimization in tool wear for friction-stir welding of Al 6061+20% Al₂O₃ MMC. *Materials Science and Engineering: A*. 2003;349(1-2):156-165.
20. Xiushuo Z, Yu'e M, Meng Y, Wei H, Yilin P, Zhenhai W. Effects of biaxial residual stress components on mixed-mode fatigue crack propagation behavior in friction stir welded 7075-T6 aluminium alloy panel. *Theoretical and Applied Fracture Mechanics*. 2022;121: 103437.
21. Belaziz A, Bouamama M, Zahaf S. Experimental Study of the Influence of the Surface Roughness on the Friction Stir Welding of FSW Joints. *Materials Proceedings*. 2022;8(1): 9.
22. Sanjay KJ, Ravi SA, Prashant P. Effect of the process parameters on the mechanical properties of the weld joint in the friction stir welding process. *International Journal of Materials Engineering Innovation*. 2022;13(2): 110-127.
23. Schmidt H, Hattel J. Heat source models in simulation of heat flow in friction stir welding. *International Journal of Offshore and Polar Engineering*. 2004;14: 296-304.
24. Song M, Kovacevic R. Thermal modeling of Friction Stir Welding in a moving coordinate system and its validation. *International Journal of Machine Tools & Manufacture*. 2002;43: 605-615.

25. Khandkar MZH, Khan JA, Reynolds AP. Prediction of temperature distribution and thermal during friction stir welding: input torque-based model. *Science and Technology of Welding and Joining*. 2003;8: 165-174.
26. Milan P, Danko LZ, Nenad K, Miroslav D, Zorana L, Miodrag H, Slobodan R, Sebastian B. Influence of Tool and Welding Parameters on the Risk of Wormhole Defect in Aluminum Magnesium Alloy Welded by Bobbin Tool FSW. *Metal*. 2022;12(6): 969.
27. Józef I, Jerzy W. Advance in Friction Stir Processed Materials. *Materials*. 2022;15(11): 3742.

THE AUTHORS

Azzeddine Belaziz 

e-mail: belaziz2013@gmail.com

Mohamed Bouamama 

e-mail: bouamamamohameddoc@gmail.com

Imane Elmequenni 

e-mail: imaneelmequenni@gmail.com

Samir Zahaf 

e-mail: samir.zahaf@univ-dbkm.dz